



Original Article

# Short-term Physical Activity Reduces Metabolic-associated Steatohepatitis by Promoting the Degradation of Branched-chain Amino Acids in Skeletal Muscle

Mingshu Gao<sup>1#</sup>, Jiaying Li<sup>1#</sup>, Yanan Zhang<sup>2</sup>, Jiangtao Huang<sup>3</sup>, Jiaqi Chen<sup>3</sup>, Dawen Liao<sup>3</sup>, Shengnan He<sup>4</sup>, Qian Bi<sup>5</sup>, Lele Ji<sup>6\*</sup> and Yulu Du<sup>3\*</sup>

<sup>1</sup>Department of Life Sciences, Northwest University, Xi'an, Shaanxi, China; <sup>2</sup>School of Medicine, Northwest University, Xi'an, Shaanxi, China; <sup>3</sup>State Key Laboratory of Cancer Biology and Department of Physiology and Pathophysiology, School of Basic Medical Science, Fourth Military Medical University, Xi'an, Shaanxi, China; <sup>4</sup>Department of Breast and Thyroid Surgery of Shenzhen Second People's Hospital, The First Affiliated Hospital of Shenzhen University, Shenzhen, Guangdong, China; <sup>5</sup>Department of Geriatric, the Fifth Medical Center, Chinese PLA General Hospital, Beijing, China; <sup>6</sup>National Demonstration Center for Experimental Preclinical Medicine Education, School of Basic Medical Science, Fourth Military Medical University, Xi'an, Shaanxi, China

Received: February 16, 2025 | Revised: April 22, 2025 | Accepted: May 08, 2025 | Published online: May 30, 2025

## Abstract

**Background and Aims:** Metabolic-associated steatohepatitis (MASH) is an advanced and progressive liver disease that potentially causes cirrhosis and hepatocellular carcinoma. Exercise is a crucial and effective intervention for ameliorating metabolic dysfunction-associated steatotic liver disease. This study aimed to provide a comprehensive understanding of the underlying mechanisms of MASH, which benefit a broad spectrum of MASH patients, including those who have difficulty engaging in physical activity. **Methods:** We established a mouse model of MASH and selectively knocked down L-type amino acid transporter 1 and alanine-serine-cysteine transporter 2. Mice were fed a high-fat high-cholesterol diet and subjected to either short- or long-term exercise regimens. We assessed the phosphorylation and activity of branched-chain alpha-keto acid dehydrogenase (BCKDH) as well as branched-chain amino acid (BCAA) content in skeletal muscle following exercise. **Results:** Short-term exercise significantly reduced hepatic steatosis and inflammation without causing notable changes in body weight. It also enhanced BCKDH activity in skeletal muscle and decreased hepatic BCAA accumulation. Muscle-specific overexpression of BCKDH further promoted BCAA catabolism and significantly attenuated hepatic steatosis and inflammation in high-fat high-cholesterol-fed mice. In contrast, muscle-specific L-type amino acid transporter 1 knockdown, which suppresses

BCAA uptake, markedly abolished these beneficial effects. Interestingly, BCKDH overexpression in muscle increased glutamine levels in both the blood and liver. Hepatic alanine-serine-cysteine transporter 2 knockdown, which inhibited glutamine uptake, lessened the protective effect of exercise on MASH. Further *in vitro* study revealed that glutamine derived from myocytes improved redox homeostasis and inhibited lipid accumulation in hepatocytes. **Conclusions:** Short-term exercise enhances BCAA catabolism in skeletal muscle and promotes glutamine production, which circulates to the liver to improve redox balance and alleviate MASH.

**Citation of this article:** Gao M, Li J, Zhang Y, Huang J, Chen J, Liao D, *et al.* Short-term Physical Activity Reduces Metabolic-associated Steatohepatitis by Promoting the Degradation of Branched-chain Amino Acids in Skeletal Muscle. *J Clin Transl Hepatol* 2025;13(7):542–554. doi: 10.14218/JCTH.2025.00072.

## Introduction

Metabolic dysfunction-associated steatotic liver disease (MASLD) is the most prevalent chronic liver disease.<sup>1</sup> It manifests as either simple steatosis or a more advanced form characterized by steatosis, inflammation, and fibrosis, known as metabolic dysfunction-associated steatohepatitis (MASH). While simple steatosis is typically benign and reversible, MASH is progressive and may lead to cirrhosis, liver failure, and hepatocellular carcinoma. Given the complex pathogenesis and heterogeneity of the disease, the only drug approved to date is the thyroid hormone receptor  $\beta$  agonist resmetirom,<sup>2</sup> which has a response rate of only 25–30% and is associated with high costs. Lifestyle interventions, particularly exercise, are critical in ameliorating MASH. For instance, exercise-mediated weight loss reduces intrahepatic triglyceride content and suppresses immune cell-driven inflammation

**Keywords:** Metabolic-associated steatohepatitis; Amino acids; Branched-chain; Exercise; Aerobic exercise; Liver-skeletal muscle crosstalk; Glutamine.

#Contributed equally to this work.

\*Correspondence to: Yulu Du, State Key Laboratory of Cancer Biology and Department of Physiology and Pathophysiology, School of Basic Medical Science, Fourth Military Medical University, No. 169 Changle West Road, Xi'an, Shaanxi 710032, China. ORCID: <https://orcid.org/0009-0004-4830-4094>. Tel: +86-19935495987, E-mail: [yuludu2022@163.com](mailto:yuludu2022@163.com); Lele Ji, National Demonstration Center for Experimental Preclinical Medicine Education, School of Basic Medical Science, Fourth Military Medical University, No. 169 Changle West Road, Xi'an, Shaanxi 710032, China. ORCID: <https://orcid.org/0000-0003-4200-7780>. Tel: +86-15829727685, E-mail: [jilele@fmmu.edu.cn](mailto:jilele@fmmu.edu.cn).

by downregulating proinflammatory cytokines.<sup>3-6</sup> However, long-term exercise remains difficult for many patients due to poor compliance. Short-term exercise has demonstrated benefits in other contexts: it improves various cognitive functions in the elderly and significantly enhances maximal oxygen uptake, diastolic blood pressure, fasting glucose, and cardiometabolic risk factors in obese individuals.<sup>7,8</sup> Nevertheless, the role and mechanisms of short-term exercise in MASH progression remain unclear, highlighting the need for further research and the identification of effective therapeutic targets.

Circulating branched-chain amino acids (BCAAs), including valine, leucine, and isoleucine, are positively correlated with hepatic cholesterol and triglyceride levels. Elevated serum BCAAs have been observed in patients with MASH,<sup>9,10</sup> at least in part due to reduced catabolism in the liver and adipose tissue. Additionally, BCAA-activated mechanistic target of rapamycin complex (mTORC) in hepatocytes is associated with insulin resistance, a condition that can be mitigated by enhanced BCAA degradation.<sup>11-13</sup> Abnormal mTORC activation also promotes *de novo* fatty acid and lipid synthesis,<sup>14</sup> contributing to hepatic steatosis. These findings illustrate a strong association between BCAA accumulation and metabolic disorders.<sup>15,16</sup> Additionally, MASH is characterized by reduced mitochondrial respiratory capacity, increased proton leakage, elevated oxidative stress, diminished antioxidant defenses, and heightened inflammatory responses, suggesting a central role for oxidative stress in its pathogenesis and progression.<sup>17,18</sup> Notably, exercise has been shown to counteract impaired BCAA catabolism in rodent and human adipose tissues by upregulating BCAA metabolic enzymes and enhancing hepatic antioxidant responses.<sup>19</sup> We hypothesize that correcting BCAA metabolic dysregulation may inhibit MASH progression by reducing hepatic oxidative stress and lipid synthesis.

## Methods

### Animal model

All mice were housed under specific pathogen-free conditions with a 12-h light/dark cycle at a room temperature of  $22 \pm 0.5^\circ\text{C}$ . Throughout the study, all mice had ad libitum access to food and water. Healthy male *C57BL/6J* mice, starting at eight weeks of age, were continuously fed a high-fat, high-cholesterol (HFHC) diet (protein, 14%; fat, 42%; carbohydrates, 44%; cholesterol, 0.2%; TP26304; Trophic Diet, Nantong, Jiangsu Province, China) for 16 weeks. Control mice received a normal diet (protein, 18.3%; fat, 10.2%; carbohydrates, 71.5%; 1,025; HuaFuKang Bioscience Co., Ltd., Beijing, China).<sup>20</sup> All animal experiments and protocols were approved by the Animal Ethics Committee of the Air Force Medical University (approval number: IA-CUC-20220351) and conducted in accordance with the National Institutes of Health Guide for the Care and Use of Laboratory Animals.

### Exercise training protocol

The exercise regimen was based on a previously established protocol.<sup>21</sup> Briefly, mice were acclimated to a motor-driven treadmill (H-PT, Zhenghua Biological Instruments, Anhui, China) for five consecutive days. They were then trained with either short-term (two weeks) or long-term (eight weeks) exercise (Fig. 1A) on a treadmill set at a  $5^\circ$  incline and a speed of 15 m/min (60 min/day, five days/week). All experiments were performed 48 h after the completion of either the two-week or eight-week training program.

### Adeno-associated virus infection

AAV2/9 containing L-type amino acid transporter 1 (LAT1) shRNA (AAV2/9-MHCK7-shLAT1), AAV8 containing ASCT2 shRNA (AAV8-ALB-shASCT2), and AAV2/9 containing branched-chain alpha-keto acid dehydrogenase (BCKDH) (AAV2/9-MHCK7-BCKDH) were purchased from WZ Biosciences Inc. (Shandong, China). To achieve muscle-specific knockdown of LAT1 and overexpression of BCKDH in *C57BL/6J* mice, AAV2/9-MHCK7-shLAT1 and AAV2/9-MHCK7-BCKDH were administered via *in situ* gastrocnemius muscle injection ( $1 \times 10^{11}$  viral genomes [VG]/mouse) at 18 weeks of age, as previously described.<sup>22</sup> AAV2/9-MHCK7-shCtrl and AAV2/9-MHCK7-GFP were used as negative controls. For liver-specific knockdown of ASCT2, AAV8-TBG-shASCT2 was delivered via tail vein injection ( $5 \times 10^{11}$  VG/mouse), with AAV8-TBG-shCtrl serving as a negative control. Infection efficiency was evaluated by Western blotting two weeks post-injection.

### Cell culture

The immortalized human hepatocyte cell line *THLE* (maintained in our laboratory) and the mouse skeletal muscle cell line *C2C12* (Cell Bank of the Type Culture Collection of the Chinese Academy of Sciences, Shanghai, China) were cultured in DMEM (PM150210, Pricella, Wuhan, China) supplemented with 10% fetal bovine serum (E600001, Sangon Biotech, Shanghai, China) and 1% penicillin-streptomycin (P1400, Solarbio, Beijing, China) at  $37^\circ\text{C}$  in a humidified incubator with 5%  $\text{CO}_2$ .

### Lentiviral infection

Cells were seeded in six-well plates at a density of  $5 \times 10^4$  cells/well and allowed to adhere overnight. The following day, the medium was removed, and *C2C12* and *THLE* cells were transduced with lentiviruses (LV) expressing BCKDH at a multiplicity of infection of 20 or with shRNA targeting ASCT2 (LV-shASCT2) at a multiplicity of infection of 10, as previously described.<sup>23</sup> After 16 h, the culture medium was replaced, and cells were incubated for an additional 32 h. Approximately 48 h post-infection, puromycin (HY-K1057, MedChemExpress, Monmouth Junction, NJ, USA) was added to the medium at a final concentration of 8–16  $\mu\text{g}/\text{mL}$ . Expression of BCKDH and ASCT2 was confirmed by western blotting in puromycin-selected cells.

### Co-culture cell model

To establish an *in vitro* hepatic steatosis model, *THLE* cells were treated with palmitic acid (PA, 0.5mM; P0500, Sigma-Aldrich, St. Louis, MO, USA) and oleic acid (OA, 1.0mM; O-1008, Sigma-Aldrich) for 18 h. Control cells were treated with 0.5% fatty acid-free BSA (GC305010, Servicebio, Wuhan, China). For co-culture, LV-BCKDH-infected *C2C12* cells were seeded in the upper chamber, while PA/OA-treated *THLE* cells were seeded in the lower chamber of a 24-well co-culture plate, as previously described.<sup>24</sup> *C2C12* cells were cultured in DMEM with 10% serum, whereas *THLE* cells were cultured in DMEM with 0.5mM PA, 1.0mM OA, and 10% serum for 18 h. Following this, media were replaced with DMEM supplemented with 10 mM BCAAs at a 2:1:1 weight ratio of leucine, valine, and isoleucine (L-leucine, 61819; L-isoleucine, 58879; L-valine, 94619; Sigma-Aldrich), and the chambers were co-cultured for an additional 12 h. Cellular glutamine content, triglyceride (TG), and total cholesterol (TC) were determined, and Oil Red O staining was performed.

### Biochemical measurements

Blood samples were collected following a 6-h fast. Serum

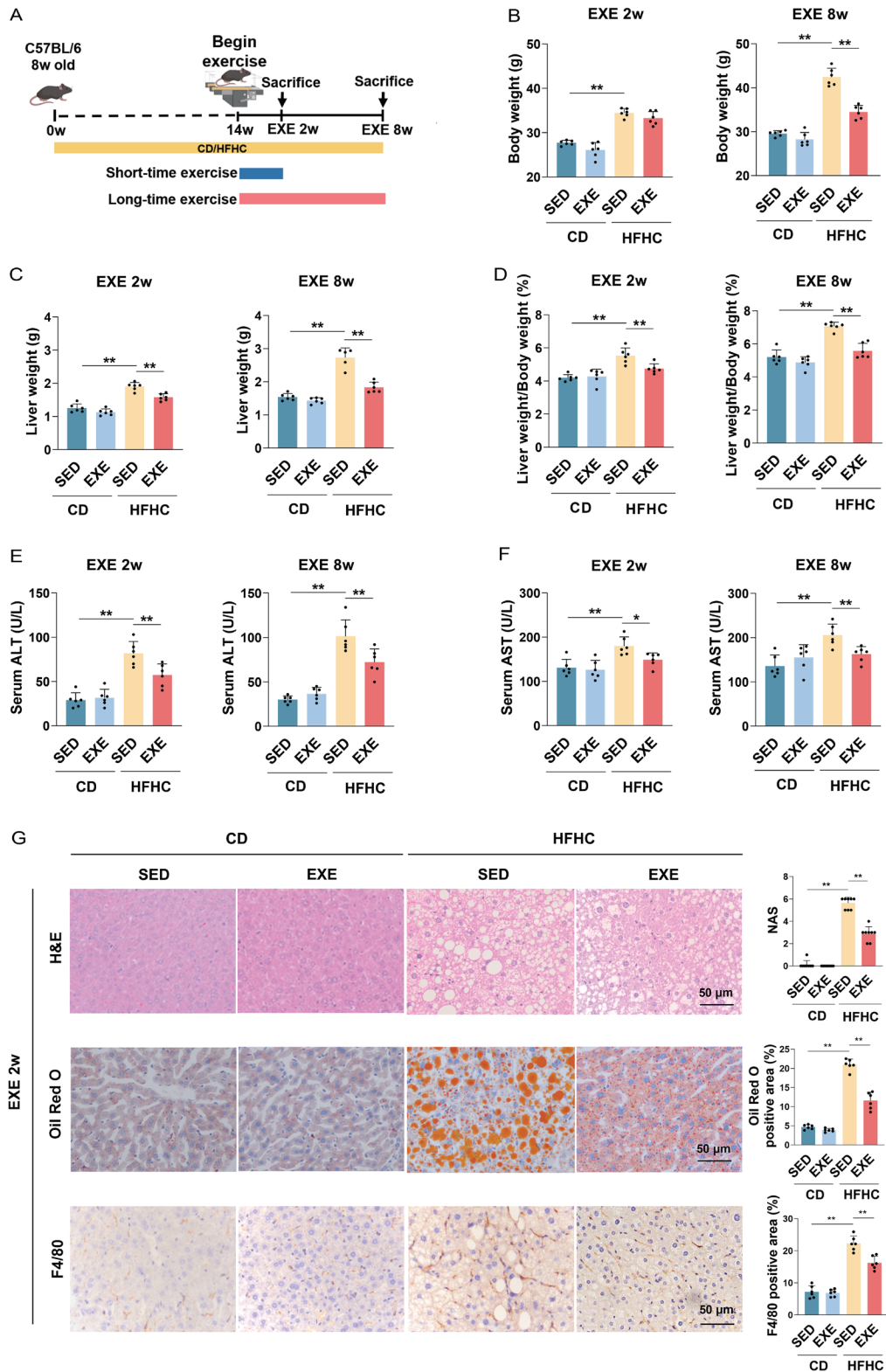


**Fig. 1. Effects of short-term exercise on MASH independent of weight loss.** (A) Schematic representation of the experimental protocol designed to evaluate the effects of two- or eight-week exercise on HFHC-induced MASH in mice. (B–F) Analyses of body weight (B), liver weight (C), liver weight-to-body weight ratio (D), and serum ALT (E) and AST (F) levels in different groups (n = 6). (G) Representative images and quantitative analyses of liver sections stained with H&E, Oil Red O, and F4/80 from different groups (n = 6). \*p < 0.05, \*\*p < 0.01. Scale bar, 50 μm. MASH, Metabolic-associated steatohepatitis; CD, control diet; HFHC, high-fat and high-cholesterol diet; SED, sedentary group; EXE, exercise group; ALT, alanine aminotransferase; AST, aspartate aminotransferase; NAS, NAFLD activity score; HE, hematoxylin-eosin.

levels of triglycerides, cholesterol, alanine aminotransferase (ALT), and aspartate aminotransferase (AST) were measured using an automatic biochemical analyzer (717000, Hitachi, Tokyo, Japan), as previously described.<sup>25</sup> Triglyceride levels in liver tissues and cells were measured using a Triglyceride Colorimetric Assay Kit (MAK266-1KT; Sigma-Aldrich).<sup>26</sup>

#### **Hematoxylin and eosin staining and immunohistochemistry**

Hematoxylin and eosin staining and immunohistochemistry were performed as previously.<sup>26</sup> Briefly, mouse tissues were fixed in 4% paraformaldehyde solution, embedded in paraffin, and sectioned at 5  $\mu$ m. The slides were stained with hematoxylin and eosin (Hematoxylin, G1004, Servicebio; Eosin, BA-4024, Baso, Zhuhai, China) and photographed under a microscope (Olympus CX31, Olympus, Nagano, Japan) to determine the NAFLD activity score (NAS).<sup>25</sup> The NAFLD activity score was calculated as the sum of the steatosis, hepatocyte ballooning, and lobular inflammation scores. Steatosis was scored from 0–3 (0, <5% steatosis; 1, 5–33% steatosis; 2, 34–66% steatosis; and 3, >67% steatosis). Hepatocyte ballooning was scored from 0–2 (0, normal hepatocytes; 1, normal-sized hepatocytes with pale cytoplasm; 2, enlarged pale hepatocytes at least twofold in size). Lobular inflammation was scored from 0–3 based on the number of inflammatory foci per 20 $\times$  field (0, none; 1, <2 foci; 2, 2–4 foci; 3,  $\geq$ 4 foci).

For immunohistochemical analysis, paraffin-embedded sections were dewaxed and incubated with anti-F4/80 antibody (GB11027, 1:1,000 dilution; Servicebio) at 4°C overnight. Anti-rabbit IgG was used as the secondary antibody. Immunohistochemical staining was visualized using a 3,3'-diaminobenzidine substrate kit (KIT-9730; MXB, Fuzhou, China). Images were acquired using a light microscope (CX43, Olympus).

#### **Oil Red O staining**

Frozen liver sections (8  $\mu$ m) or *THLE* cells in 24-well culture plates were stained with 0.5% Oil Red O (O0625; Sigma-Aldrich) for 30 min and counterstained with hematoxylin for 5 min.<sup>27</sup> Red lipid droplets were observed under a microscope.

#### **Western blotting and quantitative real-time polymerase chain reaction (RT-PCR) analysis**

Western blotting and quantitative RT-PCR were performed as previously described.<sup>28</sup> Briefly, snap-frozen tissues and cells were lysed in radioimmunoprecipitation assay buffer (AP023, AccuRef Scientific, Shaanxi, China) supplemented with a protease inhibitor cocktail (P9599, Sigma-Aldrich) and a phosphatase inhibitor (PHOSS-RO, Roche, Basel, Switzerland). Proteins were quantified using a bicinchoninic acid kit (23225, Thermo Fisher, Waltham, MA, USA), separated by 10% SDS-PAGE, and transferred to a PVDF membrane (IPVH00010, Thermo Fisher). Membranes were blocked with 5% non-fat milk in TBST and incubated overnight at 4°C with specific primary antibodies, followed by HRP-conjugated secondary antibodies. Signals were detected using an enhanced chemiluminescence kit (170-5061, Bio-Rad, Hercules, CA, USA) and imaged using a ChemiDoc MP imaging system (Bio-Rad). The antibodies used in this study (anti-BCKDH, anti-p-BCKDH, anti-S6K1, anti-p-S6K1, anti-ASCT2, anti- $\beta$ -actin, anti-4E-BP1, anti-p-4E-BP1, and anti-GAPDH) are listed in Supplementary Table 1. Total RNA was extracted using the TRI reagent (T9424, Sigma-Aldrich) and reverse-transcribed to generate complementary DNA using the Pri-

meScript RT Reagent Kit with genomic DNA Eraser (RR047A, Takara, Shiga, Japan). Quantitative RT-PCR was performed using the SYBR Premix Ex Taq II Kit (RR390A, Takara). The primers used are listed in Supplementary Table 2.  $\beta$ -actin was used as an internal control.

#### **Quantification of BCAAs**

BCAA levels were measured using a branched-chain amino acid assay kit (ab83374; Abcam, Cambridge, United Kingdom), following the manufacturer's instructions.<sup>29,30</sup> The enzymatic reaction that oxidizes and deaminates BCAAs generates NADH, which reacts with the NADH reduction probe to produce a colored product. Absorbance was measured at 450 nm using a spectrophotometer, and BCAA levels were calculated using a standard curve.

#### **Measurements of metabolite levels**

To measure tissue metabolites, approximately 10 mg of tissue was homogenized and centrifuged at 10,000  $\times$  g for 10 min. Plasma homogenates were incubated at 4°C overnight and centrifuged at 2,500  $\times$  g for 15 min. The supernatant was collected for further analysis. Glutamine levels in the lysates were quantified using a glutamine colorimetric assay kit (K556-100; BioVision, Inc., Milpitas, CA, USA).<sup>31–33</sup> Isovaleryl-CoA was quantified using a Mouse Isobutyryl-CoA ELISA Kit (YJ210684, Jiangsu Meimian Industrial, Jiangsu, China), 2-methylbutyryl-CoA was quantified using a Mouse 2-Methylbutyryl-CoA ELISA Kit (YJ410357, Jiangsu Meimian Industrial), and isobutyryl-CoA was quantified using a Mouse Isobutyryl-CoA ELISA Kit (YJ214016, Jiangsu Meimian Industrial), following the respective manufacturer's protocols.

#### **BCKDH activity assay**

BCKDH activity was quantified spectrophotometrically using a commercial assay kit (GMS50935.2, GENMED, Minneapolis, MN, USA), according to established protocols.<sup>34</sup> The BCKDH complex was extracted from fresh tissue samples using 9% polyethylene glycol. Activity was calculated by monitoring the change in absorbance at 600 nm over time and applying this to a dichlorophenol-indophenol standard curve to determine the nanomolar concentration of the product formed.

#### **In situ detection of reactive oxygen species (ROS) levels**

Cellular ROS production in hepatocytes was assessed using 2',7'-dichlorodihydrofluorescein diacetate (DCFH-DA, S0033S; Beyotime Biotechnology, Shanghai, China), as previously described.<sup>35</sup> Briefly, hepatocytes or frozen liver sections were incubated with 10  $\mu$ M DCFH-DA for 30 min at 37°C in the dark, then washed three times with 1 $\times$ PBS. Fluorescence was observed under a laser scanning confocal microscope. ImageJ software was used to quantify fluorescence intensity as follows: ImageJ was launched and the target image was opened. Channels were separated via Image > Color > Split Channels. The green channel was selected, and the threshold was adjusted using Image > Adjust > Threshold to highlight the regions of interest. Measurements were then configured and calculated. In the results window, the "Mean" value represented the average fluorescence intensity.

#### **Lipid peroxidation and glutathione (GSH)/GSSG assay**

Malondialdehyde (MDA), a marker of lipid peroxidation, was measured using an MDA assay kit (S0131S; Beyotime) as previously described.<sup>36</sup> Total GSH levels were measured us-

ing a GSH and GSSG assay kit (S0053; Beyotime), following the manufacturer's instructions.

### Statistical analyses

Data were analyzed using GraphPad Prism 9.5.1 software (San Diego, CA, USA) and were presented as the mean  $\pm$  standard error of the mean. Differences between two groups were analyzed using paired two-tailed Student's *t*-tests. For comparisons among multiple groups, one-way analysis of variance followed by the Bonferroni post hoc test was used. Statistical significance was defined as  $*p < 0.05$  and  $**p < 0.01$ .

## Results

### Short-term exercise alleviates MASH independently of weight loss

Figure 1A shows the exercise protocol. As expected, the eight-week exercise program significantly reduced body weight and markedly ameliorated the MASH phenotype (Fig. 1B–F, Supplementary Fig. 1B, C, E). Notably, although the two-week exercise program did not reduce body weight (Fig. 1B), it significantly decreased liver weight (Fig. 1C) and the liver-to-body weight ratio (Fig. 1D). Serum ALT (Fig. 1E) and AST (Fig. 1F) levels were also significantly reduced after two weeks of exercise. Histological analysis indicated that two weeks of exercise reduced hepatic steatosis and inflammatory cell infiltration and downregulated key inflammation-related genes (Fig. 1G, Supplementary Fig. 1D). Furthermore, expression of fibrosis-related genes, such as ACTA2 and TGF- $\beta$ 1, was downregulated (Supplementary Fig. 1D). In addition, hepatic TG and TC levels decreased following two weeks of exercise (Supplementary Fig. 1A). These findings suggest that the alleviation of MASH through short-term exercise is not solely mediated by energy expenditure.

### Short-term exercise ameliorates BCAA accumulation in MASH

To investigate the potential mechanisms by which short-term exercise ameliorates MASH, we analyzed liver transcriptome data from a published MASH cohort (GSE164760). KEGG pathway enrichment analysis of metabolic functions revealed that BCAA degradation pathways were among the most significantly altered in MASH tissues compared to healthy liver tissues (Fig. 2A). Elevated BCAA levels were observed in the livers of MASH mice compared to normal mice, whereas short-term exercise significantly reversed this effect (Fig. 2B). *In vitro* experiments demonstrated that BCAA treatment promoted lipid accumulation in hepatocytes (Supplementary Fig. 2A–B). BCKDH functions as the rate-limiting enzyme in BCAA catabolism (Fig. 2C). However, assessment of BCKDH mRNA and total protein expression in the livers of MASH mice revealed no significant alterations (Fig. 2C, Supplementary Fig. 2D). Previous studies have reported that hepatic BCKDH activity is significantly diminished in metabolic disorders such as MASLD, diabetes, and obesity,<sup>37,38</sup> potentially due to increased phosphorylation of BCKDH.<sup>39,40</sup> Therefore, we evaluated BCKDH phosphorylation and activity in MASH mice following exercise. Our results indicated that BCKDH phosphorylation (Fig. 2D) and enzymatic activity (Fig. 2E) were not significantly altered by exercise. Similarly, there were no significant differences in the levels of downstream BCAA metabolites (isovaleryl-CoA, 2-methylbutyryl-CoA, and isobutyryl-CoA) between the exercised and non-exercised groups (Fig. 2F). These findings suggest that exercise does not directly impact hepatic BCAA metabolism. Interestingly,

serum BCAA levels in MASH mice were significantly reduced after exercise (Fig. 2G), suggesting enhanced systemic BCAA degradation. Given that skeletal muscle is the primary site for BCAA oxidation<sup>41</sup> and that skeletal muscle metabolism is accelerated by exercise, we measured BCAA content in skeletal muscle. Surprisingly, BCAA levels in skeletal muscle increased post-exercise (Fig. 2H). No significant changes were observed in BCKDH mRNA or total protein expression in skeletal muscle (Supplementary Fig. 2D, Fig. 2I). However, BCKDH activity in skeletal muscle was significantly upregulated following exercise (Fig. 2I–J). Correspondingly, the levels of downstream metabolites of BCAA oxidation were notably increased (Fig. 2K), indicating enhanced BCAA catabolism in skeletal muscle post-exercise. These findings suggest that exercise may alleviate hepatic lipid accumulation and inflammation by activating skeletal muscle BCKDH and promoting BCAA oxidation in muscle tissue.

### Enhanced catabolism of BCAAs in muscle ameliorates MASH

To determine whether enhanced BCAA catabolism in skeletal muscle is a mechanism underlying MASH improvement after short-term exercise, we generated a muscle-specific BCKDH-overexpressing mouse model by injecting AAV2/9-MHCK7-BCKDH into *C57BL/6J* mice on either a control diet or HFHC diet. Compared to controls, AAV2/9-MHCK7-BCKDH injection significantly increased BCKDH expression (Fig. 3A) and activity (Fig. 3B) in skeletal muscle. Muscle-specific BCKDH overexpression reduced liver weight (Fig. 3C) and the liver-to-body weight ratio (Fig. 3D) in HFHC-fed mice. Biochemical analyses revealed significantly lower liver TG (Fig. 3E), liver TC (Fig. 3F), and serum ALT and AST levels (Fig. 3G–H) in these mice. Histological analysis confirmed reduced hepatic lipid accumulation and inflammatory infiltration (Fig. 3K). Additionally, mRNA levels of inflammation- and fibrosis-related genes were significantly reduced in AAV-BCKDH mice (Fig. 3I–J). These results demonstrate that enhancing BCAA catabolism in skeletal muscle significantly ameliorates MASH.

### Suppression of BCAA uptake attenuates the beneficial effects of short-term exercise on MASH

We next assessed the mRNA expression of known BCAA transporters<sup>42,43</sup> in skeletal muscle and found a significant upregulation of LAT1 (SLC7A5) following short-term exercise (Fig. 4A–B). To examine the role of LAT1, we established a muscle-specific LAT1 knockdown mouse model via AAV2/9-MHCK7-shLAT1 injection (Fig. 4C–D), which significantly reduced BCAA content in muscle tissue (Fig. 4E). These mice were then fed an HFHC diet and subjected to two weeks of exercise training. Our data revealed that LAT1 knockdown partially reversed the beneficial effects of short-term exercise on MASH. This was demonstrated by increased liver weight (Fig. 4F), a higher liver-to-body weight ratio (Fig. 4G), elevated liver TG and TC levels (Fig. 4H–I), increased serum AST and ALT (Fig. 4J), and worsened hepatic steatosis and inflammation (Fig. 4K). Furthermore, mRNA levels of inflammation- and fibrosis-related genes were upregulated (Supplementary Fig. 3C–D) in AAV2/9-MHCK7-shLAT1 mice compared to controls. These results demonstrate that suppression of BCAA uptake in muscle attenuates the beneficial effects of short-term exercise, underscoring the critical role of skeletal muscle BCAA metabolism in the amelioration of MASH.

### Muscle BCAA catabolism promotes muscle glutamine secretion and ameliorates MASH

The accumulation of BCAAs within hepatocytes activates the

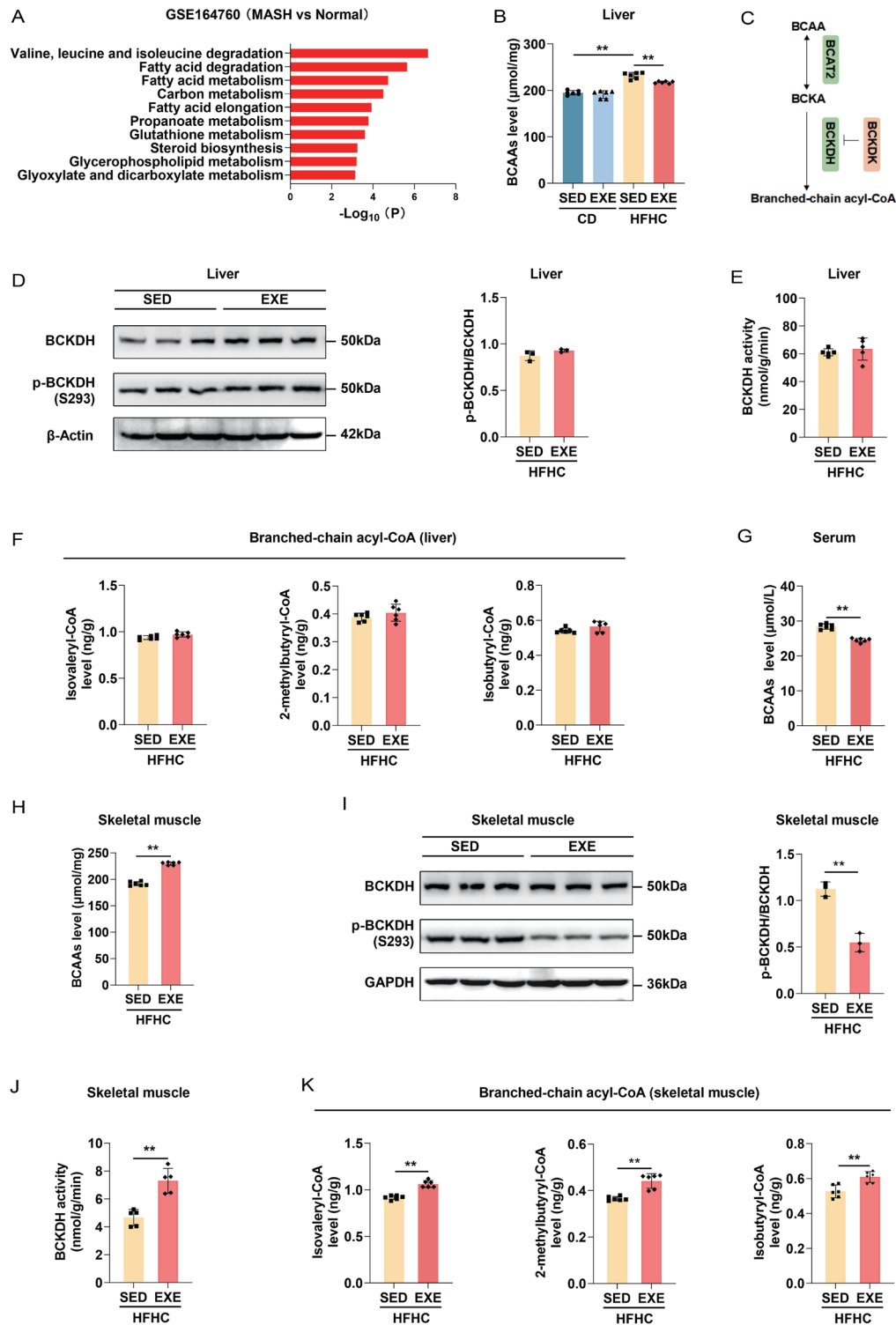


**Fig. 2. Effect of short-term exercise on BCAA accumulation in MASH.** (A) KEGG pathway analysis of differentially expressed genes in liver tissues from patients with MASH versus healthy controls. (B) Hepatic BCAA levels in mice subjected to different treatments (n = 6). (C) Schematic representation of BCAA catabolism. (D) Western blot analysis of BCKDH expression and Ser293 phosphorylation in the liver of treated mice (n = 3). (E, F) Analysis of BCKDH enzyme activity and branched-chain acyl-CoA levels in the livers of treated mice (n = 6). (G, H) BCAA levels in serum and skeletal muscle of treated mice (n = 6). (I) Western blot analysis of BCKDH expression and Ser293 phosphorylation in skeletal muscle (n = 3). (J, K) Analysis of BCKDH enzyme activity and branched-chain acyl-CoA levels in skeletal muscle (n = 6). \**p* < 0.05, \*\**p* < 0.01. KEGG, Kyoto Encyclopedia of Genes and Genomes; BCAA, branched-chain amino acid; CD, control diet; HFHC, high-fat and high-cholesterol diet; SED, sedentary group; EXE, two-week exercise group; BCAT2, Branched Chain Amino Acid Transaminase 2; BCKA, Branched-chain α-ketoacids; BCKDK, Branched Chain Keto Acid Dehydrogenase; BCKDH, Branched Chain Keto Acid Dehydrogenase Kinase.

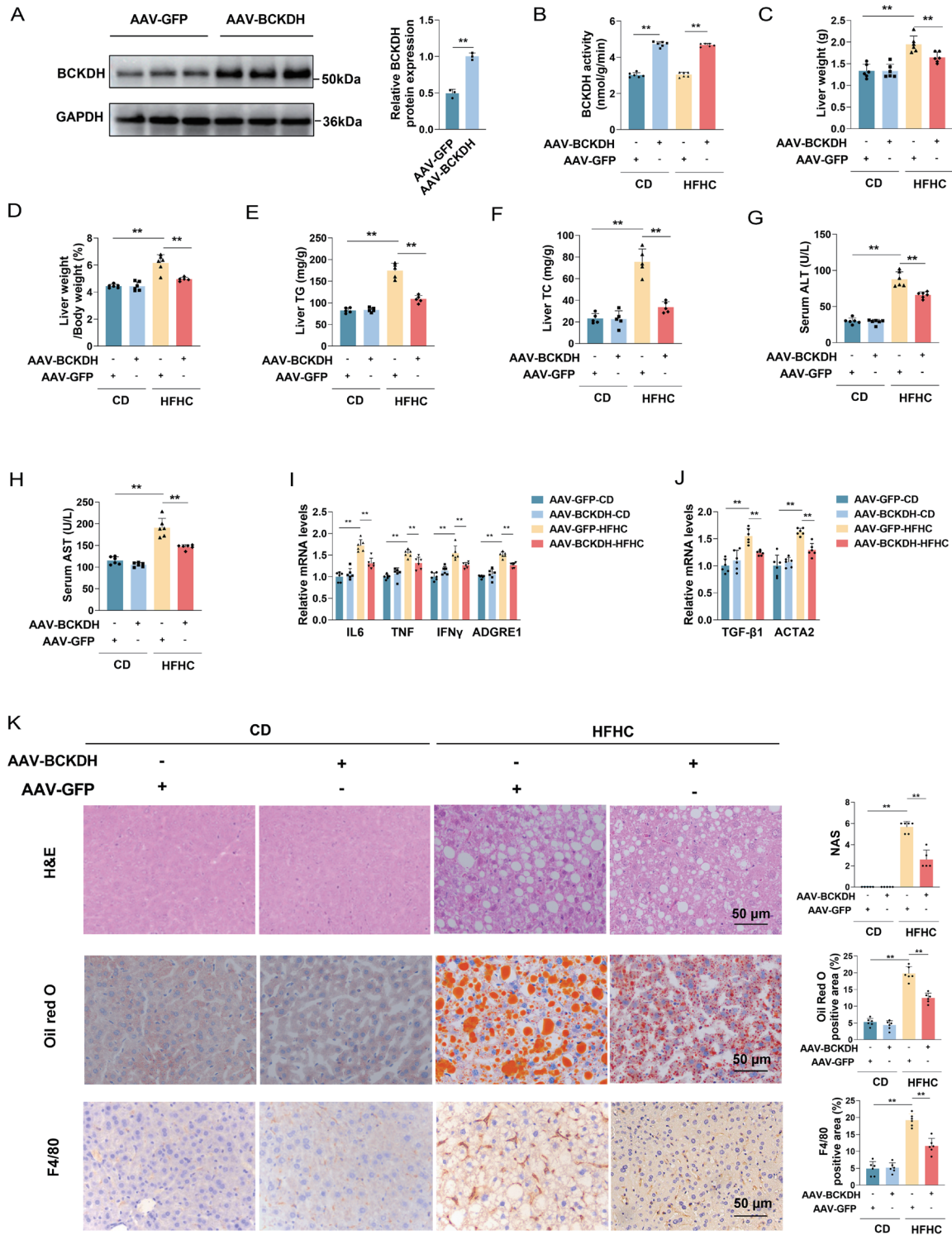


**Fig. 3. The impact of increased BCAA catabolism in skeletal muscle on MASH progression.** (A) Western blot analysis of BCKDH expression in skeletal muscle of mice injected with AAV2/9-MHCK7-BCKDH or negative control (n = 3). (B) Relative BCKDH activity in skeletal muscle (n = 6). (C–H) Measurements of liver weight (C), liver weight-to-body weight ratio (D), hepatic TG (E) and TC (F) levels, and serum ALT (G) and AST (H) levels in different groups (n = 6). (I, J) Relative mRNA expression of inflammation- and fibrosis-related genes in the liver (n = 6). (K) Representative images and quantitative analyses of liver sections stained with H&E, Oil Red O, and F4/80. \**p* < 0.05, \*\**p* < 0.01. Scale bar, 50  $\mu$ m. AAV, Adeno-Associated Virus; GFP, Green fluorescent protein; BCKDH, Branched Chain Keto Acid Dehydrogenase Kinase; CD, control diet; HFHC, high-fat and high-cholesterol diet; TG, triglyceride; TC, total cholesterol; ALT, alanine aminotransferase; AST, aspartate aminotransferase; mRNA, Messenger RNA; IL6, Interleukin-6; TNF, Tumor necrosis factor; IFN $\gamma$ , Interferon- $\gamma$ ; ADGRE1, Adhesion G Protein-Coupled Receptor E1; TGF- $\beta$ 1, Transforming Growth Factor Beta 1; ACTA2, Actin Alpha 2; NAS, NAFLD activity score; HE, hematoxylin-eosin; +, with; -, without.

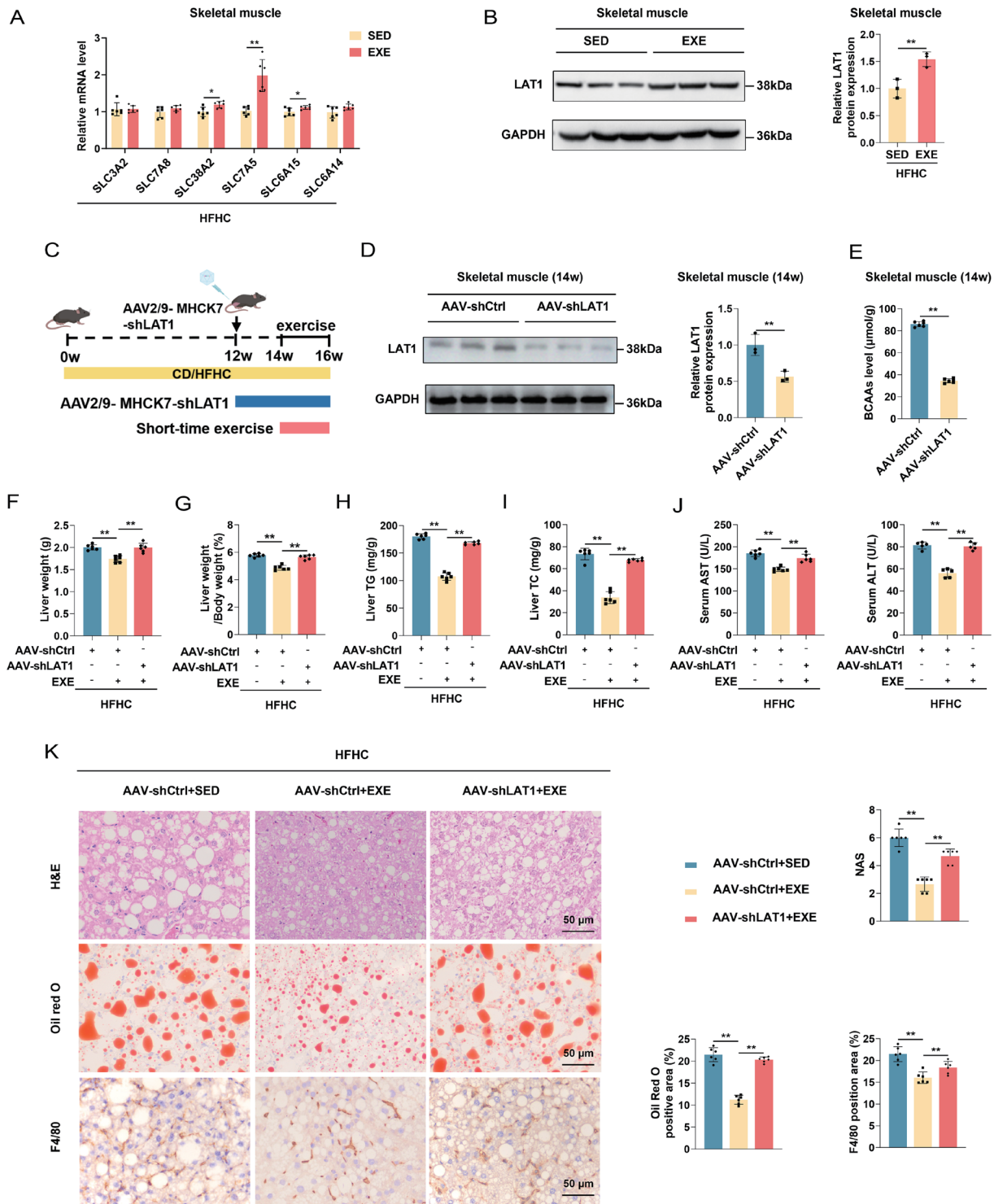


**Fig. 4. The effect of muscle BCAA uptake on exercise-induced alleviation of MASH.** (A) Relative mRNA expression of BCAA transporters in skeletal muscle ( $n = 6$ ). (B) Western blot analysis of LAT1 (SLC7A5) protein expression in skeletal muscle ( $n = 3$ ). (C) Schematic of the experimental procedure for LAT1 knockdown in skeletal muscle of HFHC-fed mice with or without exercise. (D, E) LAT1 protein expression (D) and BCAA levels (E) in skeletal muscle two weeks after AAV injection ( $n = 3$ ). (F–J) Liver weight (F), liver weight-to-body weight ratio (G), hepatic TG (H) and TC (I) levels, and serum ALT and AST (J) levels in different groups ( $n = 6$ ). (K) Representative images and quantitative analyses of liver sections stained with H&E, Oil Red O, and F4/80 ( $n = 6$ ). Scale bar, 50  $\mu\text{m}$ . \* $p < 0.05$ , \*\* $p < 0.01$ . SLC3A2, Solute Carrier Family 3 Member 2; CD, control diet; HFHC, high-fat and high-cholesterol diet; SED, sedentary group; EXE, exercise group; AAV, Adeno-Associated Virus; MHCK7, hybridized-myosin heavy chain enhancer-/muscle creatine kinase enhancer-promoter; LAT1, L-type amino acid transporter 1; GAPDH, Glyceraldehyde-3-Phosphate Dehydrogenase; shCtrl, short hairpin RNA control; shLAT1, short hairpin RNA targeting LAT1; TG, triglyceride; TC, total cholesterol; ALT, alanine aminotransferase; AST, aspartate aminotransferase; NAS, NAFLD activity score; HE, hematoxylin-eosin; +, with; -, without.

mTORC1, a central regulator of lipid homeostasis.<sup>44</sup> Notably, mTORC1 activation significantly exacerbates steatosis and inflammation in MASH models.<sup>45–47</sup> Consistent with these findings, we observed a marked increase in the phosphorylation of the mTORC1 downstream effectors p70S6K and 4E-BP1 in MASH mice (Supplementary Fig. 3A). Interestingly, short-term exercise reduced the phosphorylation of p70S6K and 4E-BP1 in the livers of MASH mice (Supplementary Fig. 3B), suggesting that short-term exercise may inhibit mTOR signaling by promoting BCAA catabolism, thereby delaying MASH progression.

To further elucidate the mechanism by which BCAA catabolism alleviates MASH, we quantified glutamine, a downstream metabolite of BCAA catabolism, in the muscle, serum, and liver tissues of HFHC-fed *C57BL/6J* mice following AAV2/9-MHCK7-BCKDH injection (Fig. 5A–B). Glutamine levels significantly increased in all three tissues, with the most pronounced elevation observed in the skeletal muscle (Fig. 5C). Subsequently, we established a co-culture system in which *THLE* hepatocytes were cultured in 24-well plates and exposed to a mixture of PA/OA to induce lipid accumulation. *C2C12* skeletal muscle cells, either overexpressing BCKDH or not, were seeded in the upper chambers of transwell plates and cultured in BCAA-containing medium (Fig. 5D, Supplementary Fig. 4A). Co-culture with BCKDH-overexpressing *C2C12* cells led to a marked elevation in glutamine concentrations in both the *THLE* cells and the corresponding culture supernatant (Fig. 5E, Supplementary Fig. 4B). Measurements of cellular TG and TC content, along with Oil Red O staining, revealed a substantial reduction in lipid accumulation in hepatocytes co-cultured with BCKDH-overexpressing muscle cells (Fig. 5F–I).

Subsequent analysis of hepatic glutamine transporter expression following short-term exercise revealed no significant alterations compared with sedentary controls (Supplementary Fig. 4C), indicating that increased hepatic glutamine influx is not mediated by upregulation of transporter expression. To assess the role of glutamine uptake, we generated a liver-specific glutamine transporter ASCT2 knockdown mouse model using AAV8-TBG-shASCT2 injection (Fig. 5J). Mice in the AAV8-TBG-shASCT2 group exhibited significantly reduced hepatic ASCT2 expression compared with the shCtrl group (Supplementary Fig. 4D–E). Knockdown of ASCT2 partially reversed the beneficial effects of short-term exercise on MASH, as evidenced by reduced hepatic glutamine content (Supplementary Fig. 4F), increased liver weight and liver-to-body ratio, elevated hepatic TG and TC levels, and increased serum AST and ALT levels (Supplementary Fig. 4G–L). Furthermore, hepatic steatosis, inflammation, and mRNA expression of inflammation- and fibrosis-related genes were significantly elevated (Fig. 5K, Supplementary Fig. 4M–N). These findings indicate that hepatic glutamine uptake is crucial for ameliorating MASH following short-term exercise.

#### **Glutamine derived from skeletal muscle may mitigate MASH by enhancing redox homeostasis**

Oxidative stress is implicated in the pathogenesis and progression of MASH. GSH is a key intracellular antioxidant, and glutamate derived from glutamine serves as a critical precursor for its synthesis.<sup>48,49</sup> We hypothesize that glutamine uptake by hepatocytes attenuates oxidative stress in MASH by promoting GSH synthesis. Our results showed that short-term exercise increased hepatic glutamine and GSH levels while reducing levels of ROS and MDA, a marker of lipid peroxidation (Fig. 6A–D). However, liver-specific knockdown of ASCT2 partially reversed these effects (Supplementary Fig. 4C, Fig. 6A–D). Similar findings were observed *in vitro*: in the

co-culture system (Supplementary Fig. 5A), ASCT2 knockdown in *THLE* cells resulted in decreased GSH levels and increased lipid accumulation, ROS, and MDA levels compared with control cells (Supplementary Fig. 5B–D, Fig. 6E–H).

#### **Discussion**

This study yielded several pivotal findings. First, short-term exercise effectively ameliorated the MASH score independent of weight loss. Second, exercise enhanced the catabolism of BCAAs in skeletal muscle, thereby reducing hepatic BCAA accumulation-associated with MASH and alleviating hepatic lipid accumulation and inflammatory cell infiltration. Third, increased BCAA catabolism in post-exercise skeletal muscle generated glutamine, which entered the bloodstream and reached the liver, thereby maintaining hepatic redox balance.

Physical exercise is recognized as a key intervention in the management of metabolic diseases. Our study demonstrated that a two-week exercise regimen significantly improved MASH scores without altering body weight. Similarly, Nayor *et al.* reported that just 12 min of intense exercise induces favorable changes in 502 metabolites associated with insulin resistance and excess adiposity, including a 2–9% reduction in BCAAs.<sup>50</sup> Furthermore, both short-term exercise and other modalities such as interval training rapidly enhance insulin sensitivity in humans.<sup>51</sup> This improvement is partly attributable to exercise-induced muscle contractions, which promote the expression and translocation of glucose transporters such as GLUT-4,<sup>52,53</sup> thereby increasing the capacity of muscle cells to uptake and utilize glucose.<sup>54,55</sup>

Abnormal BCAA accumulation is closely linked to liver disease. Our study indicates that one of the most significant metabolic alterations in the livers of MASH mice is impaired BCAA catabolism. Elevated BCAA levels were detected in both liver and serum. Similarly, Jia *et al.* identified a positive correlation between serum BCAA levels and MASLD-related indicators, including TG, total TC, ALT, and AST.<sup>56</sup> Furthermore, Grenier-Larouche *et al.* demonstrated that derivatives of the BCAA valine—such as branched-chain keto acid,  $\alpha$ -ketoisovalerate, and the branched-chain keto acid/BCAA ratio—are associated with the extent of hepatic steatosis and the development of MASH.<sup>37</sup> BCAAs also influence metabolic regulation by modulating the lipogenic transcription factor sterol regulatory element-binding protein 1, thereby increasing *de novo* fatty acid synthesis and reducing fatty acid oxidation.<sup>56</sup> Our research also revealed that short-term exercise promoted BCAA catabolism in skeletal muscle, leading to reduced BCAA levels in both serum and liver, thereby alleviating MASH. This is partially corroborated by evidence that the gut microbiota *Bacteroides stercoris* promotes MASLD progression in mice by increasing BCAA production, while reducing serum BCAA levels significantly improves MASLD.<sup>56</sup>

Skeletal muscle is the primary site of BCAA oxidation and significantly affects systemic BCAA concentrations through oxidative metabolism.<sup>41</sup> Exercise enhances this oxidative metabolism of BCAAs in the skeletal muscles. Overmyer *et al.* found that animals with greater oxidative capacity exhibited increased BCAA utilization and ATP production, mediated by the upregulation and deacetylation of proteins involved in oxidative pathways.<sup>57</sup> Blair *et al.* demonstrated that BCKDH regulation in skeletal muscle, rather than the liver, had a significant impact on fasting plasma BCAA levels in male mice.<sup>58</sup> Our study reinforces these findings by showing that short-term exercise increased BCKDH activity in skeletal muscle in MASH mice, resulting in a significant decrease in BCAA levels in both serum and liver. This reduction in BCAAs mitigated li-

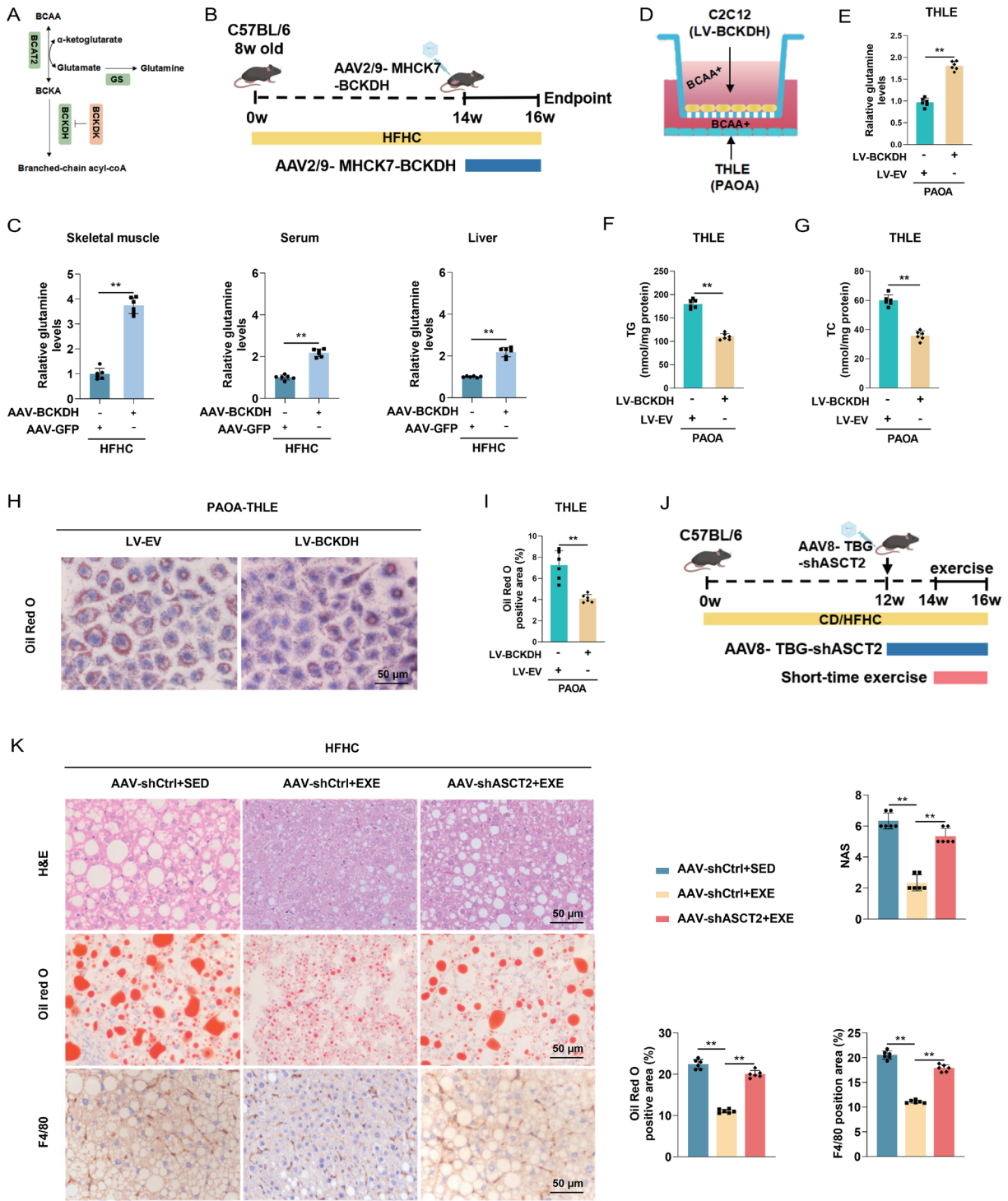


**Fig. 5. Impact of muscle BCAA catabolism-mediated glutamine secretion on MASH progression.** (A) Schematic diagram of BCAA catabolism. (B) Experimental design for BCKDH overexpression in HFHC-fed mice. (C) Relative glutamine levels in skeletal muscle, serum, and liver tissue (n = 6). (D) Co-culture of LV-BCKDH-infected C2C12 cells and PA/OA-treated THLE cells in DMEM with 10 mM BCAA. (E–G) Relative glutamine (E), cellular TG (F), and cellular TC (G) levels in THLE cells after co-culture with LV-BCKDH or LV-EV C2C12 cells (n = 6 independent experiments). (H, I) Representative images (H) and quantitative analysis (I) of Oil Red O-stained THLE cells (n = 6). (J) Experimental design for liver-specific ASCT2 knockdown in HFHC-fed mice, with or without exercise. (K) Representative images and quantitative analysis of liver sections stained with H&E, Oil Red O, and F4/80 (n = 6). \**p* < 0.05, \*\**p* < 0.01. Scale bar, 50 μm. BCAA, branched-chain amino acid; BCAT2, Branched Chain Amino Acid Transaminase 2; GS, Glutamine synthetase; BCKA, Branched-chain α-ketoacids; BCKDK, Branched Chain Keto Acid Dehydrogenase; BCKDH, Branched Chain Keto Acid Dehydrogenase Kinase; HFHC, high-fat and high-cholesterol diet; MHCK7, hybrid-myosin heavy chain enhancer-/muscle creatine kinase enhancer-promoter; SED, sedentary group; EXE, exercise group; AAV, adeno-associated virus; LV, lentivirus; EV, empty vector; PAOA, palmitic acid and oleic acid; TBG, thyroid-binding globulin; shCtrl, short hairpin RNA control; shASCT2, short hairpin RNA targeting ASCT2; NAS, NAFLD activity score; HE, hematoxylin-eosin; +, with; –, without.

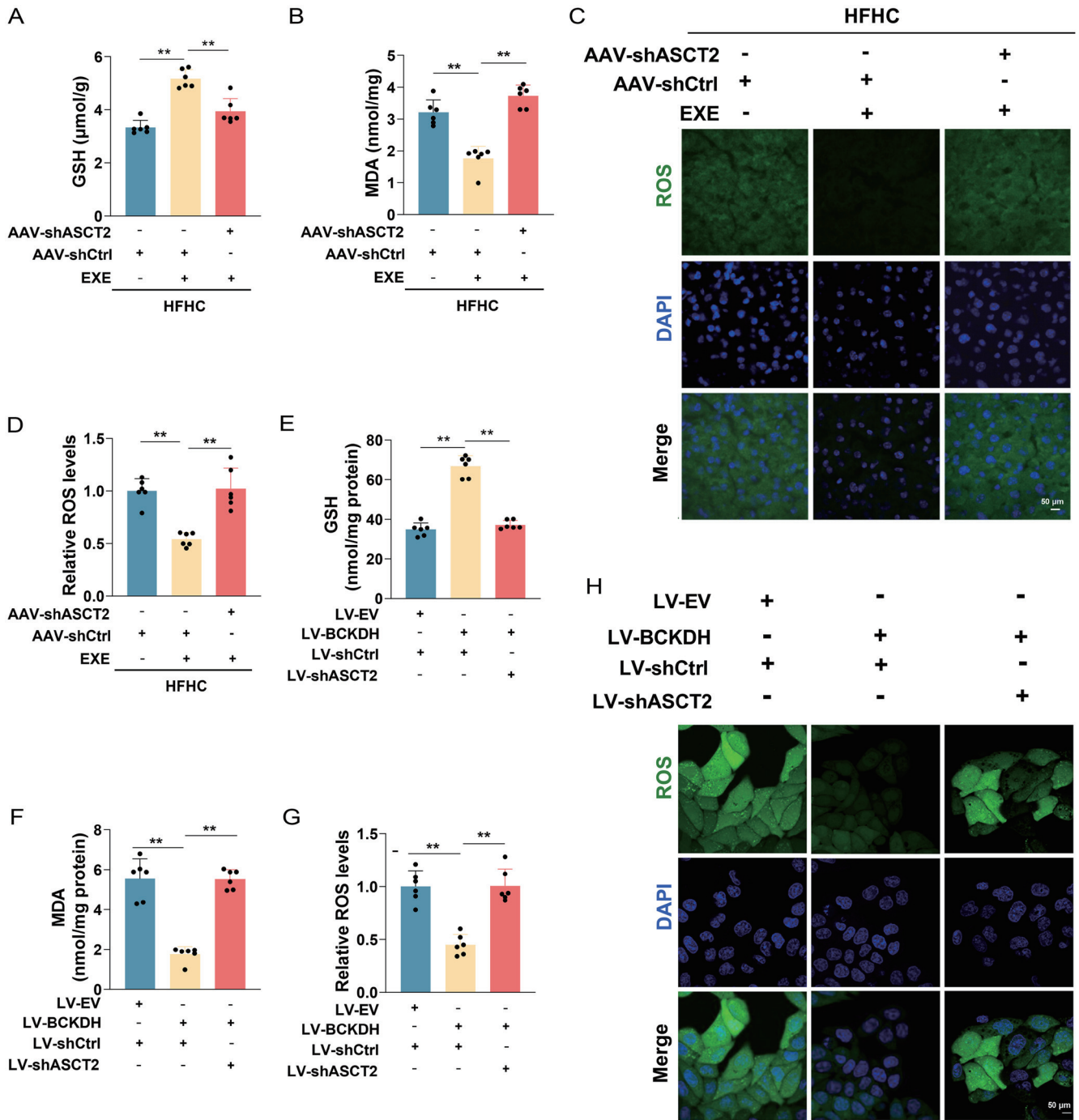


**Fig. 6. Glutamine derived from skeletal muscle regulates redox homeostasis and modulates MASH progression.** (A, B) Total glutathione (A) and MDA (B) levels in liver tissue (n = 6). (C, D) Representative images and quantitative analyses of ROS levels in liver tissue (n = 6). (E) Total glutathione in THLE cells (n = 6). (F) MDA levels in THLE cells (n = 6). (G, H) Representative images and quantitative analyses of ROS levels in THLE cells (n = 6). Scale bar, 5  $\mu\text{m}$ . Data for cell experiments are from three independent experiments. \* $p < 0.05$ , \*\* $p < 0.01$ . HFHC, high-fat and high-cholesterol diet; AAV, adeno-associated virus; LV, lentivirus; EV, empty vector. shCtrl, short hairpin RNA control; shASCT2, short hairpin RNA targeting ASCT2; ROS, reactive oxygen species; DAPI, 4',6-diamidino-2-phenylindole; GSH, Glutathione; MDA, Malondialdehyde; +, with; -, without.

pid accumulation and inflammatory cell infiltration associated with excessive hepatic BCAA levels.

Multiple studies have demonstrated beneficial effects of glutamine on liver health. For example, Shen *et al.* reported that fibroblast growth factor 15 increased the expression of

ornithine aminotransferase in hepatocytes, promoting the conversion of accumulated ornithine to glutamate. This conversion ensures a sufficient glutamate supply for ammonia detoxification via the glutamine synthesis pathway.<sup>59</sup> Moreover, inhibition of the highly expressed hepatic glutaminase

GLS1 reduces glutamine consumption, decreases hepatic lipid content, and mitigates oxidative stress in choline- and/or methionine-deficient MASH mouse models.<sup>36</sup> Among various contributing factors, oxidative stress is considered a primary driver of NAFLD progression. Excessive lipid accumulation in the liver exacerbates oxidative stress, further promoting hepatocyte steatosis and inflammatory responses.<sup>60</sup>

## Conclusions

In our study, enhanced BCAA oxidation in skeletal muscle following short-term exercise increased glutamine production, which circulated to the liver and helped ameliorate MASH by promoting redox balance. This mechanism offers a novel perspective and a promising therapeutic target for MASH treatment, with significant implications for future clinical interventions and drug development.

## Acknowledgments

We acknowledge the Analysis & Testing Laboratory for Life Sciences and Medicine at the Fourth Military Medical University for providing the essential instrumentation used in this study and the Shaanxi Provincial Innovation Capacity Enhancement Program (2023-CX-PT-33)

## Funding

This work was supported by the Key Program of the Natural Science Basic Research Plan in Shaanxi Province, China (to LJ, No. 2021JZ-28), the Shaanxi Provincial Innovation Capacity Enhancement Program (to LJ, No. 2023-CX-PT-33), the Beijing Nova Program (to QB, No. 20220484197), the Shaanxi Provincial Department of Science and Technology (to YZ, No. 2019SF-077; No. 2023KJXX-023), and the Natural Science Foundation of Guangdong Province (to SH, No. 2021A1515011426).

## Conflict of interest

The authors have no conflict of interests related to this publication.

## Author contributions

Study concept and design (MG, JL, YD), acquisition of data (MG, JL), analysis and interpretation of data (MG, JL, YZ), drafting of the manuscript (MG, JL, YZ), critical revision of the manuscript for important intellectual content (YZ, JH, JC, DL, SH, QB), administrative, technical, or material support (LJ, YD), and study supervision (LJ, YD). All authors have made significant contributions to this study and have approved the final manuscript.

## Ethical statement

All animal experiments and protocols were approved by the Animal Ethics Committee of the Fourth Military Medical University (permission number: IACUC-20220351) and conducted in accordance with the National Institutes of Health Guide for the Care and Use of Laboratory Animals. All animals received human care.

## Data sharing statement

The data supporting the findings of this study are available from the corresponding authors upon reasonable request.

## References

- [1] Mucinski JM, Salvador AF, Moore MP, Fordham TM, Anderson JM, Shryack G, *et al*. Histological improvements following energy restriction and exercise: The role of insulin resistance in resolution of MASH. *J Hepatol* 2024;81(5):781–793. doi:10.1016/j.jhep.2024.06.017, PMID:38914313.
- [2] Harrison SA, Bedossa P, Guy CD, Schattner JM, Loomba R, Taub R, *et al*. A Phase 3, Randomized, Controlled Trial of Resmetirom in NASH with Liver Fibrosis. *N Engl J Med* 2024;390(6):497–509. doi:10.1056/NEJMoa2309000, PMID:38324483.
- [3] Zhang HJ, He J, Pan LL, Ma ZM, Han CK, Chen CS, *et al*. Effects of Moderate and Vigorous Exercise on Nonalcoholic Fatty Liver Disease: A Randomized Clinical Trial. *JAMA Intern Med* 2016;176(8):1074–1082. doi:10.1001/jamainternmed.2016.3202, PMID:27379904.
- [4] Keating SE, Hackett DA, George J, Johnson NA. Exercise and non-alcoholic fatty liver disease: a systematic review and meta-analysis. *J Hepatol* 2012;57(1):157–166. doi:10.1016/j.jhep.2012.02.023, PMID:22414768.
- [5] Chalasani N, Younossi Z, Lavine JE, Diehl AM, Brunt EM, Cusi K, *et al*. The diagnosis and management of non-alcoholic fatty liver disease: practice Guideline by the American Association for the Study of Liver Diseases, American College of Gastroenterology, and the American Gastroenterological Association. *Hepatology* 2012;55(6):2005–2023. doi:10.1002/hep.25762, PMID:22488764.
- [6] Fan JG, Xu XY, Yang RX, Nan YM, Wei L, Jia JD, *et al*. Guideline for the Prevention and Treatment of Metabolic Dysfunction-associated Fatty Liver Disease (Version 2024). *J Clin Transl Hepatol* 2024;12(11):955–974. doi:10.14218/JCTH.2024.00311, PMID:39544247.
- [7] Nouchi R, Taki Y, Takeuchi H, Hashizume H, Nozawa T, Sekiguchi A, *et al*. Beneficial effects of short-term combination exercise training on diverse cognitive functions in healthy older people: study protocol for a randomized controlled trial. *Trials* 2012;13:200. doi:10.1186/1745-6215-13-200, PMID:23107038.
- [8] Batacan RB Jr, Duncan MJ, Dalbo VJ, Tucker PS, Fenning AS. Effects of high-intensity interval training on cardiometabolic health: a systematic review and meta-analysis of intervention studies. *Br J Sports Med* 2017;51(6):494–503. doi:10.1136/bjsports-2015-095841, PMID:27797726.
- [9] Glynn EL, Piner LW, Huffman KM, Slentz CA, Elliot-Penry L, AbouAssi H, *et al*. Impact of combined resistance and aerobic exercise training on branched-chain amino acid turnover, glycine metabolism and insulin sensitivity in overweight humans. *Diabetologia* 2015;58(10):2324–2335. doi:10.1007/s00125-015-3705-6, PMID:26254576.
- [10] Solon-Biet SM, Cogger VC, Pulpitel T, Wahl D, Clark X, Bagley E, *et al*. Branched chain amino acids impact health and lifespan indirectly via amino acid balance and appetite control. *Nat Metab* 2019;1(5):532–545. doi:10.1038/s42255-019-0059-2, PMID:31656947.
- [11] Lynch CJ, Adams SH. Branched-chain amino acids in metabolic signaling and insulin resistance. *Nat Rev Endocrinol* 2014;10(12):723–736. doi:10.1038/nrendo.2014.171, PMID:25287287.
- [12] White PJ, Lapworth AL, An J, Wang L, McGarrah RW, Stevens RD, *et al*. Branched-chain amino acid restriction in Zucker-fatty rats improves muscle insulin sensitivity by enhancing efficiency of fatty acid oxidation and acyl-glycine export. *Mol Metab* 2016;5(7):538–551. doi:10.1016/j.molmet.2016.04.006, PMID:27408778.
- [13] Zhou M, Shao J, Wu CY, Shu L, Dong W, Liu Y, *et al*. Targeting BCAA Catabolism to Treat Obesity-Associated Insulin Resistance. *Diabetes* 2019;68(9):1730–1746. doi:10.2337/db18-0927, PMID:31167878.
- [14] Chen M, Qiu T, Wu J, Yang Y, Wright GD, Wu M, *et al*. Extracellular anti-angiogenic proteins augment an endosomal protein trafficking pathway to reach mitochondria and execute apoptosis in HUVECs. *Cell Death Differ* 2018;25(11):1905–1920. doi:10.1038/s41418-018-0092-9, PMID:29523874.
- [15] Lian K, Du C, Liu Y, Zhu D, Yan W, Zhang H, *et al*. Impaired adiponectin signaling contributes to disturbed catabolism of branched-chain amino acids in diabetic mice. *Diabetes* 2015;64(1):49–59. doi:10.2337/db14-0312, PMID:25071024.
- [16] Lerin C, Goldfine AB, Boes T, Liu M, Kasif S, Dreyfuss JM, *et al*. Defects in muscle branched-chain amino acid oxidation contribute to impaired lipid metabolism. *Mol Metab* 2016;5(10):926–936. doi:10.1016/j.molmet.2016.08.001, PMID:27689005.
- [17] Koliaki C, Szendroedi J, Kaul K, Jelenik T, Nowotny P, Jankowiak F, *et al*. Adaptation of hepatic mitochondrial function in humans with non-alcoholic fatty liver is lost in steatohepatitis. *Cell Metab* 2015;21(5):739–746. doi:10.1016/j.cmet.2015.04.004, PMID:25955209.
- [18] Lee KC, Wu PS, Lin HC. Pathogenesis and treatment of non-alcoholic steatohepatitis and its fibrosis. *Clin Mol Hepatol* 2023;29(1):77–98. doi:10.3350/cmh.2022.0237, PMID:36226471.
- [19] Lee S, Gulseth HL, Langley TM, Norheim F, Olsen T, Refsum H, *et al*. Branched-chain amino acid metabolism, insulin sensitivity and liver fat response to exercise training in sedentary dysglycaemic and normoglycaemic men. *Diabetologia* 2021;64(2):410–423. doi:10.1007/s00125-020-05296-0, PMID:33123769.
- [20] Liu D, Zhang P, Zhou J, Liao R, Che Y, Gao M-M, *et al*. TNFAIP3 Interacting Protein 3 Overexpression Suppresses Nonalcoholic Steatohepatitis by Blocking TAK1 Activation. *Cell Metab* 2020;31(4):726–740.e728. doi:10.1016/j.cmet.2020.03.007, PMID:32268115.
- [21] Diniz TA, de Lima Junior EA, Teixeira AA, Biondo LA, da Rocha LAF, Valadão IC, *et al*. Aerobic training improves NAFLD markers and insulin resistance through AMPK-PPAR- $\alpha$  signaling in obese mice. *Life Sci* 2021;2611(1):118868. doi:10.1016/j.lfs.2020.118868.
- [22] Chi C, Fu H, Li Y-H, Zhang G-Y, Zeng F-Y, Ji Q-X, *et al*. Exerkine fibronectin type-III domain-containing protein 5/irisin-enriched extracellular

- vesicles delay vascular ageing by increasing SIRT6 stability. *Eur Heart J* 2022;43(43):4579–4595. PMID:35929617.
- [23] Zhou YX, Wei J, Deng G, Hu A, Sun PY, Zhao X, et al. Delivery of low-density lipoprotein from endocytic carriers to mitochondria supports steroidogenesis. *Nat Cell Biol* 2023;25(7):937–949. doi:10.1038/s41556-023-01160-6. PMID:37277481.
- [24] Xiao L, Mochizuki M, Wang D, Shimamura N, Sunada K, Nakahara T. Types of cell culture inserts affect cell crosstalk between co-cultured macrophages and adipocytes. *Biochem Biophys Res Commun* 2023;658:10–17. doi:10.1016/j.bbrc.2023.03.068. PMID:37011478.
- [25] Qu P, Rom O, Li K, Jia L, Gao X, Liu Z, et al. DT-109 ameliorates nonalcoholic steatohepatitis in nonhuman primates. *Cell Metab* 2023;35(5):742–757. e10. doi:10.1016/j.cmet.2023.03.013. PMID:37040763.
- [26] Ji L, Zhao Y, He L, Zhao J, Gao T, Liu F, et al. AKAP1 Deficiency Attenuates Diet-Induced Obesity and Insulin Resistance by Promoting Fatty Acid Oxidation and Thermogenesis in Brown Adipocytes. *Adv Sci (Weinh)* 2021;8(6):2002794. doi:10.1002/adv.202002794. PMID:33747723.
- [27] Hu M, Zhang D, Xu H, Zhang Y, Shi H, Huang X, et al. Salidroside Activates the AMP-Activated Protein Kinase Pathway to Suppress Nonalcoholic Steatohepatitis in Mice. *Hepatology* 2021;74(6):3056–3073. doi:10.1002/hep.32066. PMID:34292604.
- [28] Huang Q, Li J, Xing J, Li W, Li H, Ke X, et al. CD147 promotes reprogramming of glucose metabolism and cell proliferation in HCC cells by inhibiting the p53-dependent signaling pathway. *J Hepatol* 2014;61(4):859–866. doi:10.1016/j.jhep.2014.04.035. PMID:24801417.
- [29] Sánchez-González C, Nuevo-Tapioles C, Herrero Martín JC, Pereira MP, Serrano Sanz S, Ramírez de Molina A, et al. Dysfunctional oxidative phosphorylation shunts branched-chain amino acid catabolism onto lipogenesis in skeletal muscle. *EMBO J* 2020;39(14):e103812. doi:10.15252/embj.2019103812. PMID:32488939.
- [30] Yoneshiro T, Wang Q, Tajima K, Matsushita M, Maki H, Igarashi K, et al. BCAA catabolism in brown fat controls energy homeostasis through SLC25A44. *Nature* 2019;572(7771):614–619. doi:10.1038/s41586-019-1503-x. PMID:31435015.
- [31] Hu Z, Zhao TV, Huang T, Ohtsuki S, Jin K, Goronzy IN, et al. The transcription factor RFX5 coordinates antigen-presenting function and resistance to nutrient stress in synovial macrophages. *Nat Metab* 2022;4(6):759–774. doi:10.1038/s42255-022-00585-x. PMID:35739396.
- [32] Soria LR, Makris G, D'Alessio AM, De Angelis A, Boffa I, Pravata VM, et al. O-GlcNAcylation enhances CPS1 catalytic efficiency for ammonia and promotes ureagenesis. *Nat Commun* 2022;13(1):5212. doi:10.1038/s41467-022-32904-x. PMID:36064721.
- [33] Edwards DN, Ngwa VM, Raybuck AL, Wang S, Hwang Y, Kim LC, et al. Selective glutamine metabolism inhibition in tumor cells improves anti-tumor T lymphocyte activity in triple-negative breast cancer. *J Clin Invest* 2021;131(4):e140100. doi:10.1172/jci140100. PMID:33320840.
- [34] Xu C, Yang K, Xuan Z, Li J, Liu Y, Zhao Y, et al. BCKDK regulates breast cancer cell adhesion and tumor metastasis by inhibiting TRIM21 ubiquitination of talin1. *Cell Death Dis* 2023;14(7):445. doi:10.1038/s41419-023-05944-4. PMID:37460470.
- [35] Murphy MP, Bayir H, Belousov V, Chang CJ, Davies KJA, Davies MJ, et al. Guidelines for measuring reactive oxygen species and oxidative damage in cells and in vivo. *Nat Metab* 2022;4(6):651–662. doi:10.1038/s42255-022-00591-z. PMID:35760871.
- [36] Simon J, Nunez-Garcia M, Fernandez-Tussy P, Barbier-Torres L, Fernandez-Ramos D, Gomez-Santos B, et al. Targeting Hepatic Glutamine 1 Ameliorates Non-alcoholic Steatohepatitis by Restoring Very-Low-Density Lipoprotein Triglyceride Assembly. *Cell Metab* 2020;31(3):605–622. e610. doi:10.1016/j.cmet.2020.01.013. PMID:32084378.
- [37] Grenier-Larouche T, Coulter Kwee L, Deleyle Y, Leon-Mimila P, Walejko JM, McGarrath RW, et al. Altered branched-chain  $\alpha$ -keto acid metabolism is a feature of NAFLD in individuals with severe obesity. *JCI Insight* 2022;7(15):159204. doi:10.1172/jci.insight.159204. PMID:35797133.
- [38] White PJ, McGarrath RW, Grimsrud PA, Tso SC, Yang WH, Haldeman JM, et al. The BCKDH Kinase and Phosphatase Integrate BCAA and Lipid Metabolism via Regulation of ATP-Citrate Lyase. *Cell Metab* 2018;27(6):1281–1293. e1287. doi:10.1016/j.cmet.2018.04.015. PMID:29779826.
- [39] Lu G, Sun H, She P, Youn JY, Warburton S, Ping P, et al. Protein phosphatase 2Cm is a critical regulator of branched-chain amino acid catabolism in mice and cultured cells. *J Clin Invest* 2009;119(6):1678–1687. doi:10.1172/JCI38151. PMID:19411760.
- [40] Roth Flach RJ, Bollinger E, Reyes AR, Laforest B, Kormos BL, Liu S, et al. Small molecule branched-chain ketoacid dehydrogenase kinase (BDK) inhibitors with opposing effects on BDK protein levels. *Nat Commun* 2023;14(1):4812. doi:10.1038/s41467-023-40536-y. PMID:37558654.
- [41] Neinast MD, Jang C, Hui S, Murashige DS, Chu Q, Morscher RJ, et al. Quantitative Analysis of the Whole-Body Metabolic Fate of Branched-Chain Amino Acids. *Cell Metab* 2019;29(2):417–429. e414. doi:10.1016/j.cmet.2018.10.013. PMID:30449684.
- [42] Mastroberardino A, Spindler B, Pfeiffer R, Skelly PJ, Loffing J, Shoemaker CB, et al. Amino-acid transport by heterodimers of 4F2hc/CD98 and members of a permease family. *Nature* 1998;395(6699):288–291. doi:10.1038/26246. PMID:9751058.
- [43] Yan R, Zhao X, Lei J, Zhou Q. Structure of the human LAT1-4F2hc heteromeric amino acid transporter complex. *Nature* 2019;568(7750):127–130. doi:10.1038/s41586-019-1011-z. PMID:30867591.
- [44] Ricoult SJ, Manning BD. The multifaceted role of mTORC1 in the control of lipid metabolism. *EMBO Rep* 2013;14(3):242–251. doi:10.1038/embo.2013.5. PMID:23399656.
- [45] Gosis BS, Wada S, Thorsheim C, Li K, Jung S, Rhoades JH, et al. Inhibition of nonalcoholic fatty liver disease in mice by selective inhibition of mTORC1. *Science* 2022;376(6590):eabf8271. doi:10.1126/science.abf8271. PMID:35420934.
- [46] Park HS, Song JW, Park JH, Lim BK, Moon OS, Son HY, et al. TXNIP/VDUP1 attenuates steatohepatitis via autophagy and fatty acid oxidation. *Autophagy* 2021;17(9):2549–2564. doi:10.1080/1548627.2020.1834711. PMID:33190588.
- [47] Uehara K, Sostre-Colón J, Gavin M, Santoleri D, Leonard KA, Jacobs RL, et al. Activation of Liver mTORC1 Protects Against MASH via Dual Regulation of VLDL-TAG Secretion and De Novo Lipogenesis. *Cell Mol Gastroenterol Hepatol* 2022;13(6):1625–1647. doi:10.1016/j.jcmgh.2022.02.015. PMID:35240344.
- [48] Yin H, Liu Y, Dong Q, Wang H, Yan Y, Wang X, et al. The mechanism of extracellular CypB promotes glioblastoma adaptation to glutamine deprivation microenvironment. *Cancer Lett* 2024;597:216862. doi:10.1016/j.canlet.2024.216862. PMID:38582396.
- [49] Kim HH, Choi SE, Jeong WI. Oxidative stress and glutamate excretion in alcoholic steatosis: Metabolic synapse between hepatocyte and stellate cell. *Clin Mol Hepatol* 2020;26(4):697–704. doi:10.3350/cmh.2020.0152. PMID:33053940.
- [50] Naylor M, Shah RV, Miller PE, Blodgett JB, Tanguay M, Pico AR, et al. Metabolic Architecture of Acute Exercise Response in Middle-Aged Adults in the Community. *Circulation* 2020;142(20):1905–1924. doi:10.1161/circulationaha.120.050281. PMID:32927962.
- [51] Gilbertson NM, Eichner NZM, Francois M, Gaitán JM, Heiston EM, Weltman A, et al. Glucose Tolerance is Linked to Postprandial Fuel Use Independent of Exercise Dose. *Med Sci Sports Exerc* 2018;50(10):2058–2066. doi:10.1249/mss.0000000000001667. PMID:29762253.
- [52] Zisman A, Peroni OD, Abel ED, Michael MD, Mauvais-Jarvis F, Lowell BB, et al. Targeted disruption of the glucose transporter 4 selectively in muscle causes insulin resistance and glucose intolerance. *Nat Med* 2000;6(8):924–928. doi:10.1038/78693. PMID:10932232.
- [53] Douen AG, Ramlal T, Rastogi S, Bilan PJ, Cartee GD, Vranic M, et al. Exercise induces recruitment of the “insulin-responsive glucose transporter”. Evidence for distinct intracellular insulin- and exercise-recruitable transporter pools in skeletal muscle. *The Journal of biological chemistry* 1990;265(23):13427–13430. PMID:2199436.
- [54] Sylow L, Tokarz VL, Richter EA, Klip A. The many actions of insulin in skeletal muscle, the paramount tissue determining glycemia. *Cell Metab* 2021;33(4):758–780. doi:10.1016/j.cmet.2021.03.020. PMID:33826918.
- [55] Knudsen JR, Steenberg DE, Hingst JR, Hodgson LR, Henriquez-Olguin C, Li Z, et al. Prior exercise in humans redistributes intramuscular GLUT4 and enhances insulin-stimulated sarcolemmal and endosomal GLUT4 translocation. *Mol Metab* 2020;39:100998. doi:10.1016/j.molmet.2020.100998. PMID:32305516.
- [56] Ni Y, Qian L, Siliceo SL, Long X, Nychas E, Liu Y, et al. Resistant starch decreases intrahepatic triglycerides in patients with NAFLD via gut microbiome alterations. *Cell Metab* 2023;35(9):1530–1547. e1538. doi:10.1016/j.cmet.2023.08.002. PMID:37673036.
- [57] Overmyer KA, Evans CR, Qi NR, Minogue CE, Carson JJ, Chermiside-Scabbo CJ, et al. Maximal oxidative capacity during exercise is associated with skeletal muscle fuel selection and dynamic changes in mitochondrial protein acetylation. *Cell Metab* 2015;21(3):468–478. doi:10.1016/j.cmet.2015.02.007. PMID:25738461.
- [58] Blair MC, Neinast MD, Jang C, Chu Q, Jung JW, Axsom J, et al. Branched-chain amino acid catabolism in muscle affects systemic BCAA levels but not insulin resistance. *Nat Metab* 2023;5(4):589–606. doi:10.1038/s42255-023-00794-y. PMID:37100997.
- [59] Shen H, Zhou L, Zhang H, Yang Y, Jiang L, Wu D, et al. Dietary fiber alleviates alcoholic liver injury via Bacteroides acidifaciens and subsequent ammonia detoxification. *Cell Host Microbe* 2024;32(8):1331–1346. e6. doi:10.1016/j.chom.2024.06.008. PMID:38959900.
- [60] Chen Z, Tian R, She Z, Cai J, Li H. Corrigendum to “Role of oxidative stress in the pathogenesis of nonalcoholic fatty liver disease” [Free Radic. Biol. Med. 152 (2020) 116–141]. *Free Radic Biol Med* 2021;162:174. doi:10.1016/j.freeradbiomed.2020.06.011. PMID:32571642.